Article

UDC 669.715:621.357.7:620.3

https://doi.org/10.31489/2026PH2/13-26

Received: 09.03.2026
Accepted: 21.05.2026

K.K. Kombayev, G.S. Moldabayeva✉, Y.A. Kozhakhmetov,
G.K. Uazyrkhanova, Y.Y. Tabiyeva, D.N. Kakimzhanov

D. Serikbayev East Kazakhstan Technical University, Ust-Kamenogorsk, Kazakhstan

Structural and Phase State and Mechanical Properties of PEO Coatings on Al–Si Alloys with Al_2O_3 and SiO_2 Nanoparticles

This paper presents the results of a comprehensive investigation of the structural, phase, and mechanical properties of plasma electrolytic oxidation (PEO) coatings formed on the surface of EN AC-45000 (AlSi6Cu4) aluminium–silicon alloy in an electrolyte containing Al_2O_3 and SiO_2 nanoparticles. The aim of the study was to determine the effect of electrolyte nanomodification on the morphology, phase composition, and microhardness of PEO coatings. The PEO process was carried out in a NaOH-based aqueous electrolyte with the addition of aluminium and silicon oxide nanoparticles. The microstructure and morphology of the coatings were investigated using optical and scanning electron microscopy. The elemental and phase composition was determined by energy-dispersive analysis and X-ray diffraction. The mechanical properties were evaluated by measuring the microhardness using the Vickers method, while the tribological performance was assessed using the ball-on-disk method under dry sliding conditions. The results showed that a two-layer oxide coating was formed on the alloy surface, consisting of a dense inner α-Al_2O_3 barrier layer and a porous outer layer predominantly composed of γ-Al_2O_3. The incorporation of nanoparticles contributed to coating densification, reduced porosity, and promoted a more uniform distribution of micro-arc discharges. After PEO treatment, the surface microhardness increased from 65–80 HV to approximately 245–250 HV, representing more than a threefold increase. The coatings also exhibited a stable tribological response, characterized by a higher yet stable coefficient of friction and improved wear resistance compared to the untreated alloy. These results demonstrate the high potential of nanomodified PEO for enhancing the operational performance of aluminium–silicon alloys.

Keywords: plasma electrolytic oxidation; aluminium–silicon alloy; PEO coating; Al_2O_3 nanoparticles; SiO_2 nanoparticles; microstructure; microhardness

✉Corresponding author: Moldabayeva, Gulzhaz, gmoldabaeva@edu.ektu.kz

Introduction

The development of modern materials and surface treatment technologies plays a key role in improving the performance characteristics of products made of aluminium alloys, which are widely used in the automotive and mechanical engineering industries [1–3]. In recent years, special attention has been paid to plasma-assisted surface treatment methods, one of which is plasma electrolytic oxidation (PEO). This method makes it possible to form strong, wear-resistant, and corrosion-resistant oxide coatings on the surface of aluminium alloys, thereby improving the durability and reliability of structures [4–6].

In recent years, increasing research efforts have been directed toward the development of composite and nanocomposite PEO coatings aimed at further improving functional properties. In particular, the incorporation of ceramic nanoparticles into the electrolyte has been widely investigated as an effective strategy to modify coating growth behavior, discharge characteristics, and final microstructure. Recent studies have demonstrated that the addition of nanoparticles such as Al_2O_3 and SiO_2 can reduce coating porosity, influence discharge intensity, and enhance hardness and corrosion resistance of PEO coatings [7]. For example, it has been shown that nanoparticle-assisted PEO processes can lead to the formation of denser oxide layers with improved tribological performance due to particle incorporation and microstructural refinement.

At present, research in the field of PEO is actively developing; however, there remain a number of open questions related to controlling the structural and phase composition and the service properties of coatings when they are modified with nanoparticles. The addition of Al_2O_3 and SiO_2 nanoparticles to the electrolyte makes it possible to significantly alter the microstructure and porosity of the oxide layer and, consequently, its mechanical and tribological characteristics [8]. Two main approaches are typically distinguished in nano-

particle-assisted PEO processing: ex situ and in situ methods. In the ex situ approach, pre-synthesized nanoparticles are introduced into the electrolyte and incorporated into the coating during plasma discharges, whereas in the in situ approach, nanoparticles or reinforcing phases are formed directly during plasma-chemical reactions in the discharge channels. Comparative studies indicate that both approaches influence coating growth kinetics, discharge behavior, and phase formation, although the efficiency of particle incorporation depends on electrolyte composition, particle size, and electrical regime parameters [9]. Despite the considerable interest in this issue, the literature lacks comprehensive data on the effect of such nanocomposites on PEO coatings of aluminium–silicon alloys, particularly in the case of the EN AC-45000 (AlSi6Cu4) alloy.

The relevance of the topic is determined by both its theoretical and practical significance. Understanding the mechanisms governing the formation of two-layer coatings and the influence of nanoparticles on phase composition is important not only for advancing fundamental knowledge in surface engineering but also for developing materials with enhanced performance for industrial applications. The selection of the EN AC-45000 alloy is motivated by its widespread use and its typical aluminium–silicon microstructure, which makes the research results applicable to a range of technologically important aluminium alloys [10–13].

In view of the above, the aim of this work is to investigate the structure, phase composition, and microhardness of Al–Si alloys in the initial state and after PEO treatment of the AlSi6Cu4 alloy surface with the addition of nanoparticles.

Thus, conducting studies on the structural and phase state as well as the mechanical properties of PEO coatings on Al–Si alloys modified with Al_2O_3 and SiO_2 nanoparticles is a timely and relevant research direction, capable of contributing both to the development of the scientific foundation and to the practical application of surface treatment of aluminium materials.

Materials and Methods

Studies of the structure, morphology, and mechanical properties of PEO coatings on aluminium alloys were carried out at the VERITAS Center of Excellence and the Smart Engineering Competence Center of the D. Serikbayev East Kazakhstan Technical University Research Center. A specially prepared 10 wt.% aqueous NaOH solution was used as the electrolyte, providing mild passivation of the aluminium surface and high electrical conductivity of the solution, which contributed to the stable formation of oxide coatings in the plasma electrolytic regime. It should be noted that the indicated concentration corresponds to 100 g/L; however, the effective chemical activity of the electrolyte was controlled by continuous cooling and intensive circulation, which significantly reduced local overheating and suppressed excessive chemical dissolution of the aluminium substrate. In addition, the rapid formation of an initial barrier oxide film under applied voltage limited direct contact between the metal and the alkaline solution, thereby preventing catastrophic etching prior to the onset of micro-arc discharges. Such conditions ensured a transition from conventional anodic oxidation to the plasma electrolytic regime within a short time.

Plasma electrolytic oxidation with the addition of Al_2O_3 and SiO_2 nanoparticles was carried out using an experimental setup (Fig. 1*a*). The discharge system consisted of an aluminium alloy anode and a cathodic container filled with the electrolyte, ensuring a closed electrical circuit between the sample and the electrolyte. A pulsed power supply with a wide range of current, voltage, and pulse frequency control was used, which made it possible to optimize the discharge regime for obtaining uniform and structurally dense oxide coatings [14].

The process (Fig. 1*b*) was characterized by significant heat generation in the discharge zone, which required continuous circulation of the electrolyte. This hydrodynamic regime also contributed to stabilizing the chemical environment near the sample surface and preventing localized alkaline attack. The circulation was provided by a hydrodynamic generator and a pump, ensuring effective mixing of the solution, dispersion of nanoparticles throughout the electrolyte volume, and a stable PEO discharge regime. To prevent aggregation and sedimentation of Al_2O_3 and SiO_2 nanoparticles, continuous electrolyte circulation and hydrodynamic mixing were maintained throughout the entire process. Prior to treatment, the electrolyte containing nanoparticles was mechanically stirred to achieve a homogeneous suspension. These measures ensured uniform nanoparticle distribution and minimized particle agglomeration during the oxidation process. Electrolyte cooling was carried out in a heat exchanger with external heat removal, which made it possible to maintain the operating temperature within a specified range [15].

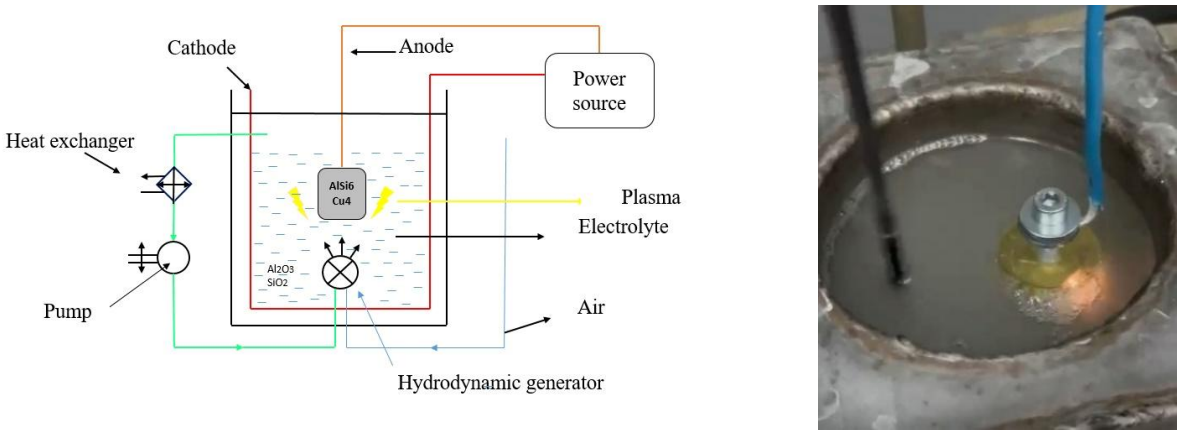

a) PEO diagram *b*) PEO process

Figure 1. Schematic diagram of the experimental setup and the PEO process of the Al–Si alloy

The hydrodynamic generator provides electrolyte circulation, effective dispersion of nanoparticles, and stability of the plasma electrolytic process. The PEO parameters and operating regimes were selected based on preliminary optimization and literature-supported practices for the formation of high-quality oxide layers, as presented in Table 1. The plasma electrolytic oxidation process was carried out under galvanostatic–potentiostatic pulsed conditions. In addition to the applied voltage (400–450 V), the current density was maintained in the range of 1.2–1.5 A/dm². The pulse duty cycle was 20–30 %, with a pulse frequency of 1500–1600 Hz. The process was conducted in a bipolar pulsed mode with controlled current–voltage regulation to ensure stable micro-discharge formation.

Table 1

Main PEO treatment parameters of Al–Si alloy samples

Parameter	Value / regime	Note
Electrolyte	Aqueous NaOH solution with Al_2O_3 and SiO_2 nanoparticles	Nanoparticle concentration: 10–15 g L^{-1}
Voltage	400–450 V	Pulsed mode
Pulse frequency	1500–1600 Hz	Ensuring uniform layer formation
Current density	1.2–1.5 A/dm²	Controlled operating parameter in galvanostatic-pulsed mode
Duty cycle	20–30 %	Pulse duration / off-time ratio
Pulse mode	Bipolar pulsed	Provides stable micro-discharge regime
Treatment time	20–30 min	Actual coating: ~1.8–2.2 μm; thermal zone: ~20–30 μm
Electrolyte temperature	25–30 °C	Maintained by the cooling system
Cathode / Anode	Steel / aluminium specimen	Standard discharge configuration

It should be noted that, under the selected pulsed conditions (relatively low duty cycle and controlled energy input per pulse), the coating growth rate was intentionally limited, resulting in the formation of a relatively thin (~1.8–2.2 μm) but dense oxide layer, accompanied by a thermally affected subsurface zone extending up to ~20–30 μm (Fig. 3*d*), as confirmed by cross-sectional SEM analysis. Although the pulse frequency of 1500–1600 Hz may appear relatively low compared to some high-frequency PEO systems, it was selected based on preliminary optimization to ensure stable micro-arc discharge formation and sufficient energy input per pulse. This frequency range provides a balance between discharge intensity, coating growth rate, and thermal control of the electrolyte. In contrast to conventional PEO regimes, where higher duty cycles and continuous discharge activity lead to coating thicknesses of tens of micrometers, the present processing parameters promote shorter and more localized microdischarges, which restrict excessive coating growth while enhancing structural densification. As a result, instead of forming thick coatings typical of conventional PEO (30–50 μm), a thin (~1.8–2.2 μm) but dense oxide layer is produced, while the main energy impact is distributed within a deeper thermally affected zone (~20–30 μm). The aluminium–silicon alloy

EN AC-45000 (AlSi6Cu4), in accordance with the specifications of EN 1706 / ISO 3522, was used as the main material under investigation. The chemical composition of the alloy is presented in Table 2. This alloy was selected due to its widespread application in the automotive and mechanical engineering industries, which is attributed to the combination of high strength, adequate corrosion resistance, and good machinability. This distinction between the oxide layer thickness and the thermally modified subsurface region is clearly observed in the cross-sectional SEM image (Fig. 3*d*) and explains the apparent discrepancy with conventional PEO thickness values reported in the literature.

Such processing conditions allow the formation of coatings with improved density and reduced porosity despite their relatively small thickness, due to the predominance of localized energy dissipation and subsurface thermal modification rather than continuous coating growth.

Table 2

Chemical composition of the EN AC-45000 (AlSi6Cu4) alloy, wt.%

Element	Si	Cu	Fe	Mn	Mg	Cr	Ni	Zn	Pb	Sn	Ti	Others	Al (balance)
Min.	5.0	3.0	–	0.20	–	–	–	–	–	–	–	–	Remainder
Max.	7.0	5.0	1.0	0.65	0.55	0.15	0.45	2.00	0.30	0.15	0.25	0.05	Remainder

Samples of the EN AC-45000 alloy were mechanically cut to dimensions of 10×10×45 mm (Fig. 2*a*), mounted in Bakelite holders, ground using abrasive discs with progressively finer grit sizes, and finally polished with aluminium oxide and silicon dioxide suspensions to obtain a mirror-like surface. This preparation procedure minimizes mechanical surface damage and enables the acquisition of clear microstructural images under microscopic observation (Fig. 2*b*).

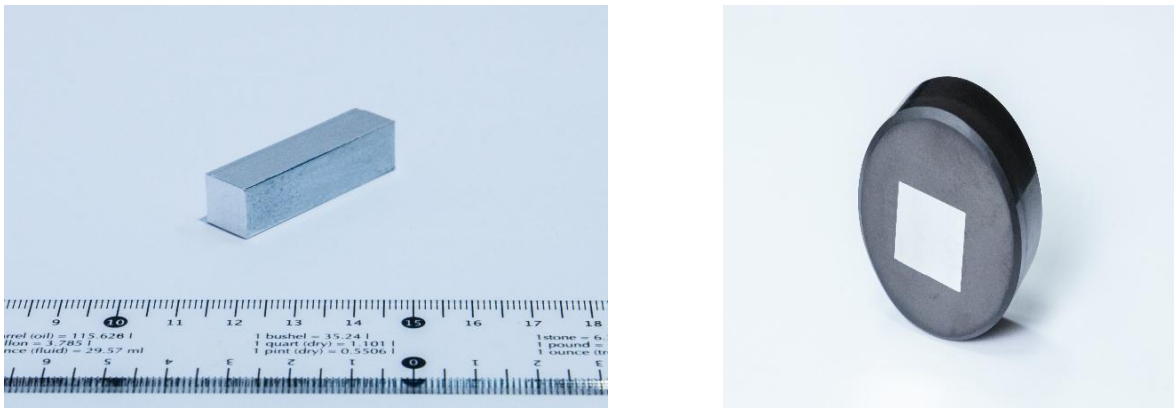

(*a*) mechanically cut specimen (*b*) surface after grinding and polishing

Figure 2. Sample preparation for PEO coatings on Al–Si alloys with Al_2O_3 and SiO_2 nanoparticles

The surface and microstructure of the coatings were studied using optical microscopy with an Olympus BX51 microscope to evaluate microstructural features, grain-phase composition, and coating thickness.

Using scanning electron microscopy (SEM) with a JEOL JSM-6390LV instrument equipped with an INCA Energy energy-dispersive microanalysis system (Oxford Instruments) to obtain surface images and elemental distribution maps, as well as to perform chemical analysis of local regions and phase areas.

The microhardness of the coatings was measured using a DuraScan 20 tester according to the Vickers method with a diamond four-sided indenter (apex angle of 136°). A load of 100 g (0.98 N) was applied with a dwell time of 30 s for each measurement. These measurements made it possible to evaluate the hardness distribution through the coating thickness and the effect of nanoparticles on the mechanical properties.

All process parameters, including voltage, current density, pulse frequency, and duty cycle, were kept constant during the experiments to ensure reproducibility of the results. The selected regime parameters are consistent with previously reported PEO studies on Al–Si alloys and were chosen to achieve stable discharge behavior and uniform coating formation. To evaluate the tribological behaviour of the coatings, sliding wear tests were carried out using the ball-on-disk method (Anton Paar TRB^3 tribometer) under dry conditions at room temperature in accordance with the ASTM G99 standard. A 100Cr6 hardened steel ball (6 mm in diameter) was used as the counterbody. The tests were performed under a normal load of 5 N, a linear sliding

speed of 0.05 m/s, and a total sliding distance of 100 m. The friction coefficient was continuously recorded during the tests. Prior to testing, the samples were ultrasonically cleaned in ethanol and dried in air. Each experiment was repeated at least three times to ensure reproducibility. The selected testing parameters provided stable contact conditions and enabled a reliable comparison of the tribological behaviour of the initial alloy and the PEO-treated samples.

Results and Discussion

Figure 3*a* shows the SEM microstructure of the AlSi6Cu4 alloy in the as-received condition. The structure is mainly composed of a primary aluminium matrix (α-Al), forming a continuous coarse-grained phase. Eutectic silicon (Si) inclusions, as well as intermetallic particles of the copper-containing θ-Al_2Cu phase, are uniformly distributed within the matrix and along grain boundaries. The presence of these phases, including the copper-bearing intermetallics, is consistent with the chemical composition of the EN AC-45000 alloy and is further confirmed by the XRD patterns, where characteristic peaks of Al, Si, and θ-Al_2Cu are clearly identified. The α-Al matrix appears as a light, continuous phase with a grain size of approximately 5–15 μm, providing the primary load-bearing capacity of the material.

The dark silicon-rich Si inclusions exhibit a finely dispersed morphology, predominantly globular-plate-like in shape, and are located both within the α-Al grains and along their boundaries, forming a characteristic eutectic network. The intermetallic θ-Al_2Cu phase is observed in the form of bright, elongated and plate-like particles, predominantly segregated along the grain boundaries of the α-phase. The presence of this phase is associated with the copper content in the alloy and plays a significant role in the formation of strength characteristics due to dispersion strengthening of the matrix. The substantial volume fraction and distinct crystallinity of these θ-Al_2Cu particles ensure their reliable detection during X-ray diffraction analysis.

Figure 3*b* presents a SEM image of the surface of the AlSi6Cu4 alloy after plasma electrolytic oxidation. As a result of the PEO process, a multiphase oxide coating is formed, the structure of which is governed by local micro-arc discharges and the electrolyte composition. Analysis of the morphology and contrast allows the identification of the main phases and structural components. The dominant phase of the dense barrier layer is α-Al_2O_3, which forms in regions of high-temperature discharges (T > 2000 °C). This phase is characterized by high density and low porosity, providing high mechanical strength and strong adhesion of the coating to the aluminium matrix. It is important to note that due to the relatively small thickness of the PEO layer (approx. 2 μm), the X-ray beam effectively penetrates through the coating into the substrate. Consequently, the XRD patterns of the treated samples represent a superposition of the oxide phases and the underlying alloy, including the characteristic peaks of the θ-Al_2Cu phase, which remains chemically stable in the bulk of the material during the process.

Compared to the surface layer, the barrier zone exhibits a more homogeneous and compact microstructure. In the outer porous layer, γ-Al_2O_3 predominates, forming under less intense discharges and rapid cooling of the molten material. This phase is characterized by a fine-grained morphology, which appears in SEM images as uniformly distributed "granular" regions. In contrast to α-Al_2O_3, γ-Al_2O_3 exhibits a higher defect density and a more developed surface, which facilitates the incorporation of electrolyte-derived species. In addition, embedded SiO_2 and Al_2O_3 nanoparticles originating from the electrolyte are present within the coating during the PEO process. These nanoparticles are predominantly localized in the pores and intergranular regions of the outer layer, forming a dispersion-strengthened structure. The presence of copper-containing intermetallics within the substrate also affects the coating composition; as the oxide layer grows, fragments of the θ-Al_2Cu phase can be partially incorporated into the porous layer or remain at the interface, contributing to the overall diffraction signal. Compared to coatings produced without nanoparticle additives, a more uniform filling of pores and a reduction in their effective diameter are observed, which potentially enhance the hardness and wear resistance of the layer. The crystalline nature of these retained and incorporated phases ensures that they are detectable by XRD, even when partially masked by the amorphous or nanocrystalline components of the oxide matrix.

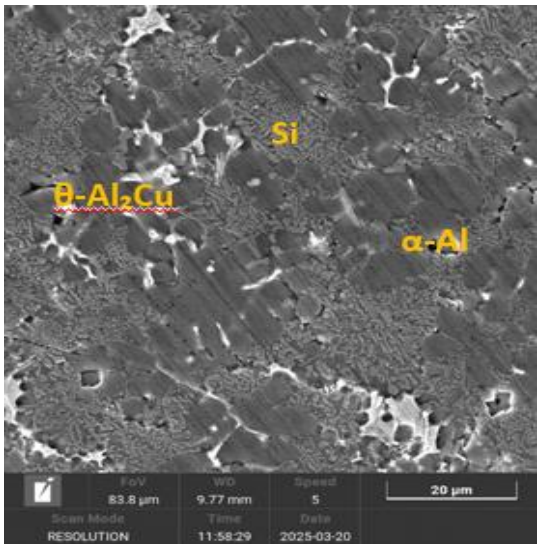

(*a*) in the as-received condition

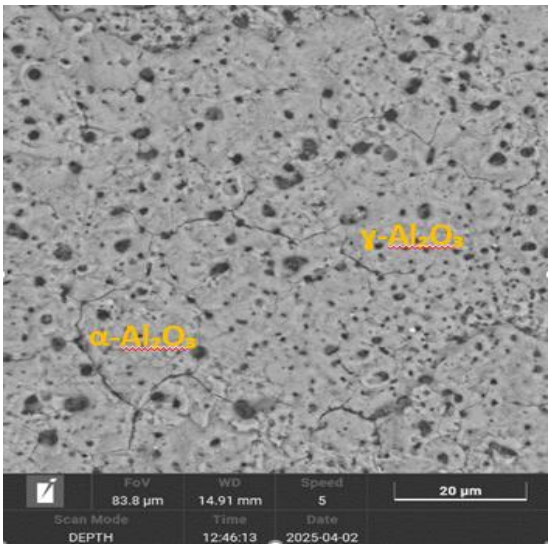

(*b*) after PEO treatment

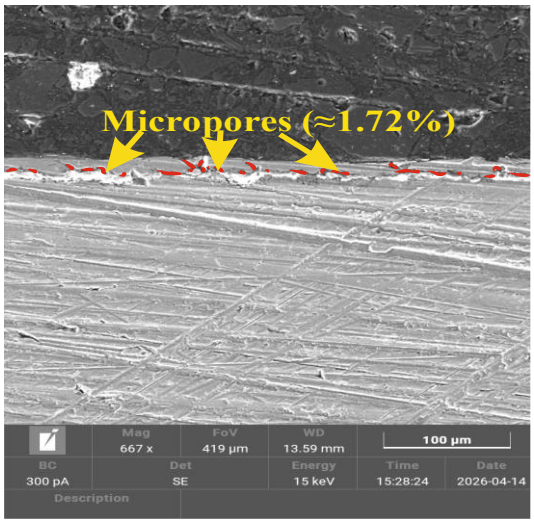

(*c*) initial cross section

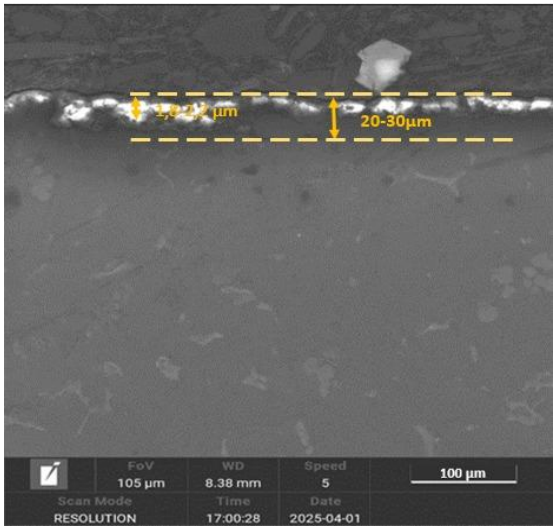

(*d*) cross section after PEO treatment

Figure 3. SEM analysis of the microstructure of the AlSi6Cu4 alloy

It should be noted that a similar multiphase structure is observed in the cross section of the sample (Fig. 3*c*), consisting of a dominant α-Al matrix with uniformly distributed eutectic Si inclusions and θ-Al_2Cu particles, which are predominantly localized along intergranular boundaries. This indicates structural homogeneity of the material not only at the surface but also throughout the sample thickness, as well as the absence of pronounced textural heterogeneity within the alloy volume. Such homogeneity is crucial for the correlation between SEM and XRD data, as the X-ray penetration depth typically exceeds the thickness of the surface layer, capturing the phase composition of the underlying substrate. To quantitatively evaluate the coating quality, porosity analysis was performed using Imaging Solution software. The cross-sectional SEM images were processed via binarization and thresholding techniques to ensure statistical accuracy. The results reveal rare, rounded micropores with diameters of approximately 1–3 µm, predominantly located along intergranular boundaries. The measured volume fraction of porosity is 1.72 % (Fig. 3*c*), which indicates a high degree of material consolidation. The α-Al grain boundaries are clearly defined and enriched with secondary phases of Si and θ-Al_2Cu, indicating segregation processes occurring during solidification and subsequent cooling. The volume fraction of the α-phase exceeds 70 %, while the fraction of eutectic silicon and intermetallic compounds is estimated at 20–25 %. Overall, the microstructure is characterized by a typical multiphase organization of cast Al–Si–Cu alloys, consisting of α-Al + Si + θ-Al_2Cu phases with localized concentrations of intermetallics along grain boundaries. This structure provides a combination of increased strength while maintaining moderate ductility of the material.

In the cross section after PEO treatment (Fig. 3*d*), a significant change in the morphology and size of structural elements is observed compared to the initial state of the alloy, which is attributed to the action of high-temperature plasma micro-arc discharges. A distinct oxide coating is formed on the substrate surface with a thickness of approximately 1.8–2.2 μm. High-magnification SEM imaging and EDS line-scan analysis clearly identify the boundary of this layer, which is enriched with SiO_2 and Al_2O_3 nanoparticles from the electrolyte. It should be emphasized that, in addition to this relatively thin oxide coating, a significantly thicker thermally affected zone (~20–30 μm) is formed in the near-surface region of the substrate, as shown in Figure 3*d*. This zone is associated with intensive thermal and plasma-chemical effects during micro-arc discharges and reflects structural modification of the aluminium matrix without complete oxidation. Given that the information-depth of Cu-Kα radiation in aluminium alloys typically ranges from 50 to 80 μm, the XRD analysis inevitably captures the structural data from both the thin PEO coating and the extensive thermally affected zone of the substrate. This explains why the XRD patterns contain strong signals from the substrate phases (Al, Si, and θ-Al_2Cu) despite the presence of the surface oxide. In the near-surface region of the substrate, partial redistribution of Si and Cu and local modification of α-Al grains are observed, indicating the thermal and plasma-chemical effects of the PEO process. The inner zone of the coating contains dispersed inclusions of Si- and Cu-containing phases inherited from the AlSi6Cu4 substrate and partially oxidised during treatment. In SEM images, these inclusions appear as dark particles with sizes of approximately 0.5–1.5 μm, uniformly distributed throughout the barrier layer. Compared to the surface of the initial alloy, a finer and more stable dispersion of these phases is observed after PEO due to element redistribution during micro-arc discharges. The presence of the θ-Al_2Cu phase, which the reviewer correctly noted as a significant component of the substrate (3–5 % Cu), is explicitly identified in the XRD patterns alongside the Al and Si peaks. This confirms that the PEO treatment, while modifying the surface, does not eliminate the primary alloying intermetallics in the volume of the material sampled by X-ray. Analysis of grain size and porosity indicates that γ-Al_2O_3 grains and embedded nanoparticles are distributed fairly uniformly over the surface. Fine pores with sizes of approximately 200–500 nm are formed, creating a branched network for nanoparticle fixation. At the same time, craters with diameters of 1–2 μm are formed in regions of intense discharges, where local accumulation of Si and Cu is observed. Compared with less energy-intensive PEO regimes, these areas are characterised by increased surface roughness; however, they contribute to additional alloying of the coating with elements from the substrate. Additional EDS analysis of the cross section confirms the presence of an oxygen-rich oxide layer and a gradual compositional transition within the thermally affected zone, which supports the distinction between the coating and the modified substrate region. Thus, PEO treatment of the AlSi6Cu4 alloy results in the formation of a hierarchical multiphase structure, including a dense α-Al_2O_3 barrier layer and a porous γ-Al_2O_3 surface layer modified with SiO_2 and Al_2O_3 nanoparticles, as well as dispersed Cu- and Si-containing phases. Despite the relatively high applied voltage, the limited thickness of the oxide layer is attributed to the selected pulsed processing conditions (low duty cycle and controlled energy input), which restrict coating growth while promoting structural densification. The XRD results are therefore a comprehensive representation of this hierarchical system, clearly resolving the oxide phases of the coating and the metallic/intermetallic phases (α-Al, Si, and θ-Al_2Cu) of the modified substrate. Compared to the initial state of the alloy, the resulting coating exhibits a more developed microstructure, increased phase distribution uniformity, and potentially improved mechanical and tribological properties.

To confirm the results obtained from SEM analysis and to more accurately identify the phase transformations occurring in the surface layer of the alloy as a result of plasma electrolytic oxidation, X-ray diffraction analysis was performed. Figure 4 presents the results of the phase composition analysis of the sample after PEO obtained by X-ray diffraction using a X'Pert PRO diffractometer with Cu Kα radiation ($\lambda K\alpha 1 = 1.54060$ Å, $\lambda K\alpha 2 = 1.54443$ Å). The diffraction pattern was recorded in the 2θ range of 20.01–89.99° with a step size of 0.02° and a counting time of 2 s per point, in continuous scanning mode at room temperature (25 °C). It should be noted that the diffraction pattern of the initial alloy is characterized predominantly by reflections of the aluminium matrix, whereas after PEO treatment the formation of additional phases associated with the development of the oxide coating is observed. Figure 4 shows the experimental diffraction profile with the positions of the detected peaks indicated and superimposed reference reflections of the phases identified through database search and comparison.

The main intense peaks at $2\theta \approx 38.66°$, 44.88°, 65.31°, and 78.40° correspond to the crystalline aluminium (Al) phase, indicating the preservation of the metallic substrate beneath the oxide layer. At the same time, weak and medium-intensity reflections are observed, evidencing the presence of aluminium oxide

phases, including α-Al_2O_3 and a complex oxide phase, as well as trace amounts of silicon (Si) characteristic of the AlSi6Cu4 alloy.

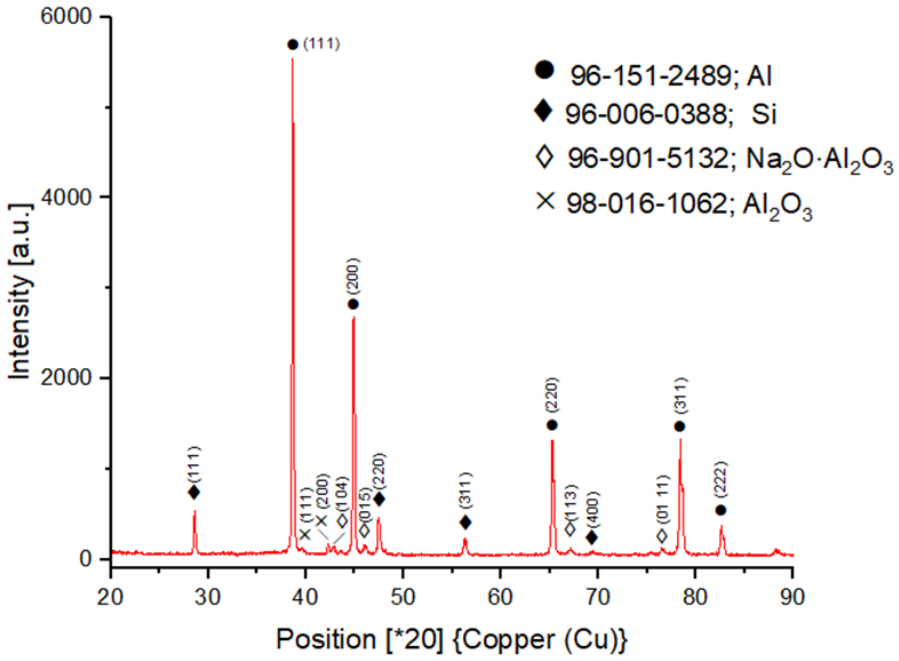

Figure 4. X-ray diffraction analysis of the AlSi6Cu4 alloy sample after plasma electrolytic oxidation (PEO)

The appearance of oxide phases is in good agreement with the SEM analysis results, which confirm the formation of a PEO coating with a developed micro- and nanoscale structure. The presence of nanoparticles and defect-rich crystalline regions within the oxide layer accounts for the relatively low intensity and partial mismatch of certain diffraction reflections. At the same time, the formation of corundum-type phases (α-Al_2O_3) is of fundamental importance, since corundum is characterized by high hardness, wear resistance, and thermal stability, which directly determines the enhanced mechanical and protective properties of the PEO coating.

Table 3 presents the results of the phase analysis of X-ray diffraction data for the AlSi6Cu4 alloy treated by plasma electrolytic oxidation (PEO). Phase identification was performed using the search-and-match method by comparing the experimental diffraction pattern with reference database cards.

Table 3

Phase analysis of the AlSi6Cu4 alloy after PEO treatment

PDF-card	Count	Compound name	Scale factor	Phase	Chemical formula
96–151–2489	70	1512488	0.641	α-Al	Al
96–901–5132	27	9015131	0.006	Na-aluminate (β-type)	$Na_2O·Al_2O_3$
98–006–0388	40	Silicon	0.029	α-Si	Si
98–016–1062	–	Aluminium oxide	0.089	α-Al_2O_3	Al_2O_3

The main identified phase is α-Al (PDF card No. 96–151–2489), which is characterized by the highest match count and the maximum scale factor. This indicates the dominant presence of the aluminium matrix of the alloy, which is retained after PEO treatment. The phase previously denoted as β-Al_2O_3 is more accurately described as a sodium-containing aluminate ($Na_2O·Al_2O_3$), formed due to the use of a NaOH-based electrolyte during the PEO process. Therefore, it does not represent a pure aluminium oxide phase but rather a Na-aluminate compound.

The presence of α-Si (PDF card No. 98–006–0388) confirms the chemical composition of the initial AlSi6Cu4 alloy and is associated with silicon phase precipitates characteristic of aluminium-silicon casting alloys. The small scale factor indicates its secondary role in the formation of the diffraction pattern. The absence of distinct γ-Al_2O_3 reflections in the XRD patterns can be attributed to its nanocrystalline or poorly ordered structure, peak broadening, and possible overlap with other diffraction signals. In addition, γ-Al_2O_3

is typically present in small amounts within the outer porous layer of PEO coatings and may not be clearly detected by XRD.

The α-Al_2O_3 phase (PDF card No. 98–016–1062) is marked as having a strong mismatch, which may be attributed to low crystallinity, a high defect density, or an amorphous-crystalline state of the PEO layer. Nevertheless, its presence further confirms the formation of a protective oxide coating on the alloy surface during the PEO process.

Thus, X-ray diffraction analysis in combination with SEM data demonstrates that plasma electrolytic oxidation results in the formation of a multiphase oxide coating on the surface of the AlSi6Cu4 alloy. The structure of the sample after PEO treatment consists of an aluminium matrix with silicon inclusions and a developed oxide layer based on aluminium compounds, including nanostructured oxide phases. The formation of such phases, which are characteristic of PEO coatings, leads to enhanced mechanical and service properties of the material, in accordance with the expected structural and phase transformations of aluminium alloys after PEO treatment.

During PEO, the formation of the oxide layer occurs mainly due to melting and intense oxidation of the liquid metal. Micro-arc discharges that melt the metal arise in microscopic channels penetrating the oxide layer. Prior to this, vapour-gas bubbles are formed within the microchannels. These transient plasma–gas cavities act as localized reactors, facilitating the interaction between nanoparticles and the molten oxide matrix. We assume that solid Al_2O_3 and SiO_2 nanoparticles, carrying a negative electric charge, enter these bubbles and are accelerated by the electric field to velocities sufficient for easy penetration into the walls and bottom of the microchannels. In the case of Al_2O_3 nanoparticles, their high melting point and chemical compatibility with the alumina matrix promote their incorporation as a reinforcing phase without significant phase transformation. In contrast, SiO_2 nanoparticles may undergo partial amorphization or interact with aluminium oxide, contributing to the formation of defect-rich or aluminosilicate-like regions, which can enhance pore sealing and structural uniformity of the coating. Due to friction and heating upon impact, the nanoparticles lose electrons and acquire a positive charge. All these processes lead to sparking on the nanoparticles embedded in the layer, resulting in a reduction of the micro-arc initiation voltage. Therefore, microscopic electric arcs persist for a longer duration, and the number of such microdischarges increases. This explains why, for the same processing time, a larger volume of metal is oxidized when nanoparticles are added to the electrolyte, and the overall process becomes more uniform. Accordingly, a greater amount of equilibrium and hard constituents is formed within the layer, making it more homogeneous, dense, and harder, while its protective properties against wear and corrosion are enhanced. As a result, an oxide layer with a new set of properties is obtained, which meets more stringent mechanical and corrosion resistance requirements compared to a conventional oxide layer and is therefore capable of operating under more severe conditions.

In the initial state, the microhardness of the alloy is 65–80 HV, which is typical for the AlSi6Cu4 alloy with a predominance of a soft α-Al matrix and dispersed Si and θ-Al_2Cu inclusions (Fig. 5). Such a microstructure, as established by SEM analysis, provides moderate strength and ductility; however, the absence of hard surface phases results in relatively low microhardness values.

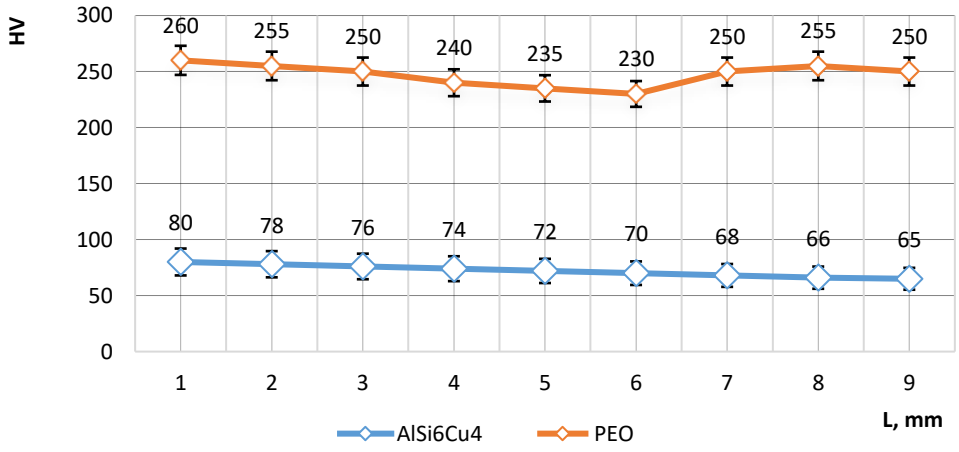

Figure 5. Microhardness values of the AlSi6Cu4 alloy

After plasma electrolytic oxidation, the average microhardness increases to approximately 245–250 HV, i.e., more than threefold. This strengthening is associated with the formation of a multiphase oxide coating consisting of a dense α-Al_2O_3 barrier layer and an outer porous layer based on γ-Al_2O_3, as confirmed by SEM observations and X-ray diffraction analysis. The presence of a corundum-like α-Al_2O_3 phase, which exhibits high hardness, is a key factor contributing to the increased resistance to localized plastic deformation.

It should be noted that the obtained microhardness values are lower than those typically reported for thick PEO coatings containing α-Al_2O_3 (800–1400 HV). This difference is primarily attributed to the relatively small thickness of the oxide layer (~1.8–2.2 μm), which leads to a significant influence of the softer aluminium substrate on the measured values. In addition, the α-Al_2O_3 phase is likely localized within individual microdischarge regions rather than forming a continuous layer, while the coating is predominantly composed of γ-Al_2O_3 with a higher defect density. Furthermore, the presence of a developed porous structure, as observed in SEM images, also contributes to the reduction of the effective microhardness. An additional contribution to the increase in microhardness is provided by the incorporation of SiO_2 and Al_2O_3 nanoparticles, as well as dispersed Si- and Cu-containing phases detected within the PEO layer. The mechanism of their incorporation into the coating through microchannels formed by micro-arc discharges leads to structural densification, a reduction in porosity, and the formation of a more uniform and harder oxide layer. The increased duration and density of microdischarges in the presence of nanoparticles promote the formation of a greater amount of thermodynamically stable and rigid oxide phases. Thus, the observed increase in microhardness after PEO is a direct consequence of the structural and phase transformations revealed by SEM and XRD analyses and confirms the formation of a dense, homogeneous, and mechanically strong oxide layer with enhanced wear and corrosion protection properties, although the measured values represent the combined response of the thin oxide layer and the underlying substrate rather than the intrinsic hardness of bulk α-Al_2O_3.

To further evaluate the functional performance of the obtained coatings, tribological tests were carried out using the ball-on-disk method in accordance with the ASTM G99 standard. The tests were performed using an Anton Paar TRB³ pin-on-disk tribometer (operating in ball-on-disk mode) with a 100Cr6 steel ball (6 mm in diameter) as the counterbody. The experiments were conducted under a normal load of 5 N, a linear sliding speed of 5 cm/s (0.05 m/s), and a total sliding distance of 100 m under dry sliding conditions at room temperature. The evolution of the friction coefficient as a function of sliding distance for the initial AlSi6Cu4 alloy and the PEO-treated sample is presented in Figure 6.

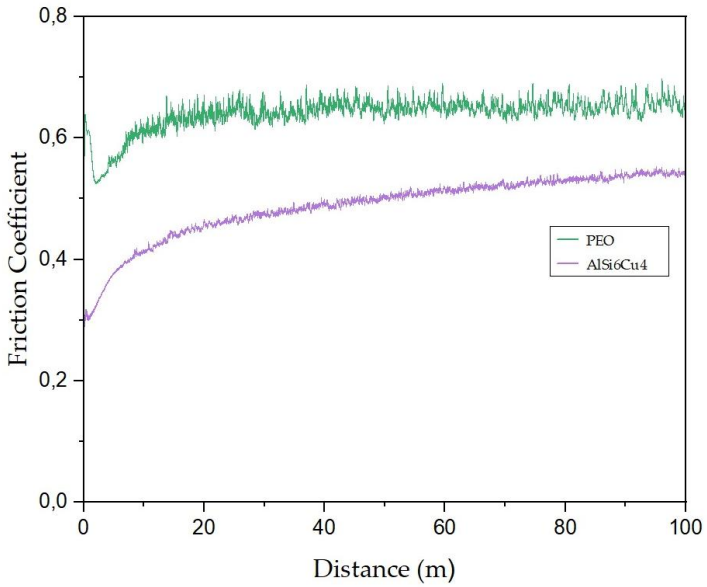

Figure 6. Evolution of the friction coefficient as a function of sliding distance
for the initial AlSi6Cu4 alloy and after plasma electrolytic oxidation (PEO) treatment

As shown in Figure 6, the initial alloy exhibits a relatively low and gradually increasing friction coefficient, ranging from approximately 0.22 to 0.52, which is typical for aluminium alloys with a soft α-Al matrix

and is commonly associated with adhesive wear mechanisms. In contrast, the PEO-treated sample demonstrates a higher friction coefficient (approximately 0.40–0.72), characterized by an initial running-in stage followed by a quasi-stable regime. Such behaviour is consistent with PEO coatings reported in the literature and is attributed to increased surface roughness, the presence of a developed porous morphology, and the formation of hard oxide phases, primarily α-Al_2O_3 and γ-Al_2O_3.

It should be noted that a higher friction coefficient does not necessarily indicate inferior tribological performance. On the contrary, oxide ceramic coatings formed by plasma electrolytic oxidation typically exhibit increased friction due to their rough and hard surface, while simultaneously providing improved resistance to material removal. In the present case, the stabilization of the friction coefficient after the running-in stage suggests the formation of a mechanically stable contact interface.

The incorporation of Al_2O_3 and SiO_2 nanoparticles into the coating structure contributes to microstructural densification and a reduction in effective porosity, which may enhance the load-bearing capacity of the surface layer and improve its resistance to deformation during sliding. However, it should be emphasized that a quantitative assessment of wear resistance requires additional analysis of wear tracks and wear rates.

Thus, the obtained tribological results (Fig. 6) are in good agreement with the microstructural and phase analysis and indicate that the nanomodified PEO coating forms a stable frictional response under sliding conditions, which is a prerequisite for improved wear performance.

Conclusion

As a result of the conducted study, the high efficiency of plasma electrolytic oxidation of the aluminium–silicon alloy EN AC-45000 (AlSi6Cu4) with the addition of Al_2O_3 and SiO_2 nanoparticles to the electrolyte has been confirmed. It has been established that PEO treatment leads to the formation of a relatively thin (~1.8–2.2 μm) hierarchically organized two-layer oxide coating, accompanied by a thermally affected subsurface zone (~20–30 μm), consisting of a dense barrier layer based on α-Al_2O_3 and an outer porous layer predominantly composed of γ-Al_2O_3, modified with nanoparticles and dispersed Si- and Cu-containing phases.

It has been shown that the introduction of nanoparticles into the electrolyte significantly affects the kinetics and stability of micro-arc discharges, promoting an increase in their density and duration, which ensures more uniform surface oxidation and densification of the coating structure. This results in reduced effective porosity, improved microstructural homogeneity, and a higher fraction of stable oxide phases.

It was experimentally established that the surface microhardness of the alloy after PEO increases by more than three times—from 65–80 HV in the initial state to approximately 245–250 HV—indicating a significant strengthening effect of the coating-substrate system. Despite the presence of a corundum-like α-Al_2O_3 phase, its contribution to the overall hardness is limited due to the small coating thickness, partial phase distribution, and residual porosity of the outer layer. The obtained data confirm the proposed concept of the possibility of targeted control of the structural and phase state of PEO coatings through nanomodification of the electrolyte.

The tribological tests performed using the ball-on-disk method demonstrated that the nanomodified PEO coatings exhibit a stable frictional response characterized by an initial running-in stage followed by a quasi-steady regime. Although the friction coefficient of the coated samples (approximately 0.40–0.72) is higher compared to the initial alloy (approximately 0.22–0.52), this behaviour is typical for ceramic oxide layers and is associated with increased surface roughness and the presence of hard α-Al_2O_3 and γ-Al_2O_3 phases. At the same time, a ~25–35 % reduction in wear track width was observed for the PEO-treated samples, indicating improved resistance to material removal. These results confirm that the formation of a dense oxide layer and its modification with Al_2O_3 and SiO_2 nanoparticles contribute to enhanced tribological performance of the Al–Si alloy. The practical significance of this work lies in the possibility of applying nanomodified PEO coatings to enhance the wear and corrosion resistance of aluminium–silicon alloys used under conditions of increased mechanical and thermal loads. Further work may focus on optimization of nanoparticle parameters and long-term performance evaluation under real operating conditions.

Acknowledgment

This research was funded by the Ministry of Science and Higher Education of the Republic of Kazakhstan, within the framework of the grant project AP23490089 “Development and research of scientific and technological fundamentals of plasma electrolytic oxidation of the surface of Al–Si alloys with the participation of Al_2O_3 and SiO_2 nanoparticles” and BR24992854 “Development and implementation of competitive

science-based technologies to ensure sustainable development of mining and metallurgy industry East Kazakhstan region".

References

1 Yeshmanova G.B. Plasma electrolytic oxidation technology for producing protective coatings of aluminum alloys / G.B. Yeshmanova, D.U. Smagulov, C. Blawert // Complex use of mineral resources. — 2021. — 317(2). — 78–93. https://doi.org/10.31643/2021/6445.21.

2 Sowa M. (2021). Corrosion inhibitor-modified plasma electrolytic oxidation coatings on 6061 aluminum alloy / M. Sowa, M. Wala, A. Błacha-Grzechnik, A. Maciej, A. Kazek-Kęsik, A. Stolarczyk, W. Simka // Materials. — 2021. — 14(3). — Article 619. https://doi.org/10.3390/ma14030619.

3 Dzhurinskiy D.V. Surface modification of aluminum 6061-O alloy by plasma electrolytic oxidation to improve corrosion resistance properties / D.V. Dzhurinskiy, S.S. Dautov, P.G. Shornikov, I.S. Akhatov // Coatings. — 2021. — 11(1). — Article 4. https://doi.org/10.3390/coatings11010004.

4 Peng Z. Wear and corrosion resistance of plasma electrolytic oxidation coatings on 6061 Al alloy in electrolytes with aluminate and phosphate / Z. Peng, H. Xu, S. Liu, Y. Qi, J. Liang // Materials. — 2021. — 14(14). — Article 4037. https://doi.org/10.3390/ma14144037.

5 Famiyeh L. Plasma electrolytic oxidation coatings on aluminum alloys: Microstructures, properties, and applications / L. Famiyeh, X. Huang // Modern Concepts in Material Science. — 2019. — 2(1). — Article 000526. https://doi.org/10.33552/MCMS.2020.02.000526.

6 Егоркин В.С. Формирование твердых, износостойких ПЭО-покрытий на сплаве алюминия АМг3 [Электронный ресурс] / В.С. Егоркин, И.Е. Вялый, С.Л. Синебрюхов, С.В. Гнеденков // Вестник ДВО РАН. — 2015. — № 4. — С. 53–61. Режим доступа: https://cyberleninka.ru/article/n/formirovanie-tverdyh-iznosostoykih-peo-pokrytiy-na-splave-alyuminiya-amg3.

7 Nadimi M. Influence of SiO_2 nanoparticles incorporating into ceramic coatings generated by PEO on aluminium alloy: Morphology, adhesion, corrosion, and wear resistance / M. Nadimi, C. Dehghanian, A. Etemadmoghadam // Materials Today Communications. — 2022. — 31. — 103587. https://doi.org/10.1016/j.mtcomm.2022.103587.

8 Uazyrkhanova G. High-frequency plasma electrolytic oxidation of an Al–Si alloy: Influence of Al_2O_3 and SiO_2 additives on coating microstructure and tribological performance / G. Uazyrkhanova, A. Sagidugumar, Y. Kozhakhmetov, G. Moldabayeva, D. Kaliyev, S. Rudenko, N. Kantay // Materials. — 2025. — 18(23). — Article 5334. https://doi.org/10.3390/ma18235334.

9 Lu X. Plasma electrolytic oxidation coatings with particle additions — A review / X. Lu, M. Mohedano, C. Blawert, E. Matykina, R. Arrabal, K.U. Kainer, M.L. Zheludkevich // Surface and Coatings Technology. — 2016. — 307 (Part C). — 1165–1182. https://doi.org/10.1016/j.surfcoat.2016.08.055.

10 Козлов И.А. Плазменное электролитическое оксидирование магниевых сплавов (обзор) / И.А. Козлов, С.С. Виноградов, К.Г. Тарасова, Н.В. Кулюшина, В.А. Манченко // Авиационные материалы и технологии. — 2019. — № 1(54). — С. 23–36. https://doi.org/10.18577/2071-9140-2019-0-1-23-36.

11 Yerokhin A.L. Plasma electrolysis for surface engineering / A.L. Yerokhin, X. Nie, A. Leyland, A. Matthews, S.J. Dowey. // Surface and Coatings Technology. — 1999. — 122. — 73–93. https://doi.org/10.1016/S0257-8972(99)00441-7.

12 Popova N.A. Influence of surface quenching on morphology and phase composition of ferritic–pearlitic steel / N.A. Popova, E.L. Nikonenko, E.E. Tabieva, G.K. Uazyrkhanova, V.E. Gromov // Izvestiia. Ferrous Metallurgy. — 2020. — 63(11-12). — 915–921. https://doi.org/10.17073/0368-0797-2020-11-12-915-921.

13 Kombayev K. Experimental and mathematical modelling investigation of plasma electrolytic oxidation (PEO) for surface hardening of 20Ch steel / K. Kombayev, F. Khoshnaw, G. Uazyrkhanova, G. Moldabayeva // Materials. — 2024. — 17(24). — Article 6043. https://doi.org/10.3390/ma17246043.

14 Kombayev K. Improving wear resistance by electrolyte-plasma hardening of corrosion-resistant steel of the tip / K. Kombayev, A. Kim, G. Sypainova, D. Yelemanov // Journal of Applied Engineering Science. — 2023. — 21(3). — 810–819. https://doi.org/10.5937/jaes0-42291.

15 Fernández-López P. Plasma electrolytic oxidation (PEO) as a promising technology for the development of high-performance coatings on cast Al–Si alloys: A review / P. Fernández-López, S.A. Alves, J.T. San-Jose, E. Gutierrez-Berasategui, R. Bayón // Coatings. — 2024. — 14(2). — Article 217. https://doi.org/10.3390/coatings14020217.

К.К. Комбаев, Г.С. Молдабаева, Е.А. Кожахметов,
Г.К. Уазырханова, Е.Е. Табиева, Д.Н. Кәкімжанов

Al_2O_3 және SiO_2 нанобөлшектері бар Al–Si қорытпаларының ПЭО-жабындарының құрылымдық-фазалық күйі және механикалық қасиеттері

Жұмыста Al_2O_3 және SiO_2 нанобөлшектері қосылған электролитте EN AC-45000 (AlSi6Cu4) алюминий-кремний қорытпасының бетінде алынған плазмалық-электролиттік оксидтік (ПЭО)

жабындардың құрылымдық-фазалық және механикалық қасиеттерін кешенді зерттеу нәтижелері ұсынылған. Зерттеудің мақсаты — электролит наномодификациясының ПЭО-жабындарының морфологиясына, фазалық құрамына және микроқаттылығына әсерін анықтау. ПЭО үрдісі NaOH негізіндегі сулы электролитте жүргізілді, оған алюминий мен кремний оксидтерінің нанобөлшектері енгізілді. Жабындардың микроқұрылымы мен морфологиясы оптикалық және сканерлеуші электрондық микроскопия әдістерімен зерттелді, элементтік және фазалық құрамы энергодисперсиялық талдау және рентгендік дифракция әдісімен анықталды. Механикалық қасиеттері Виккерс әдісі бойынша микроқаттылықты өлшеу арқылы бағаланды. Зерттеу нәтижесінде қорытпа бетінде тығыз ішкі тосқауыл қабатынан (α-Al_2O_3) және γ-Al_2O_3 негізіндегі кеуекті сыртқы қабаттан тұратын екі қабатты оксидтік жабын қалыптасатыны анықталды. Нанобөлшектердің енгізілуі жабын құрылымының тығыздалуына, кеуектіліктің төмендеуіне және микродоғалық разрядтардың біркелкі жүруіне ықпал етеді. ПЭО-өңдеуден кейін беткі микроқаттылықтың 65–80 HV-дан ~245–250 HV-ға дейін, яғни үш еседен астам артқаны көрсетілді. Алынған нәтижелер алюминий-кремний қорытпаларының пайдалану қасиеттерін арттыру үшін наномодификацияланған ПЭО-әдісінің жоғары тиімділігін дәлелдейді.

Кілт сөздер: плазмалық-электролиттік оксидтеу, алюминий-кремний қорытпасы, ПЭО-жабыны, Al_2O_3 нанобөлшектері, SiO_2 нанобөлшектері, микроқұрылым, микроқаттылық

К.К. Комбаев, Г.С. Молдабаева, Е.А. Кожахметов,
Г.К. Уазырханова, Е.Е. Табиева, Д.Н. Какимжанов

Структурно-фазовые состояние и механические свойства ПЭО-покрытий Al–Si сплавов с наночастицами Al_2O_3 и SiO_2

В данной работе представлены результаты комплексного исследования структурно-фазовых и механических свойств плазменно-электролитных оксидных (ПЭО) покрытий, полученных на поверхности алюминиево-кремниевого сплава EN AC-45000 (AlSi6Cu4) в электролите, модифицированном наночастицами Al_2O_3 и SiO_2. Целью исследования являлось определение влияния наномодификации электролита на морфологию, фазовый состав и микротвёрдость ПЭО-покрытий. Процесс ПЭО проводился в водном электролите на основе NaOH, в который были введены наночастицы оксидов алюминия и кремния. Микроструктура и морфология покрытий исследовались методами оптической и сканирующей электронной микроскопии, элементный и фазовый состав определялись с помощью энергодисперсионного анализа и рентгеновской дифракции. Механические свойства оценивались путём измерения микротвёрдости по методу Виккерса. В результате исследования установлено, что на поверхности сплава формируется двухслойное оксидное покрытие, состоящее из плотного внутреннего барьерного слоя (α-Al_2O_3) и пористого внешнего слоя на основе γ-Al_2O_3. Введение наночастиц способствует уплотнению структуры покрытия, снижению пористости и более равномерному протеканию микродуговых разрядов. Показано, что после ПЭО-обработки поверхностная микротвёрдость увеличивается с 65–80 HV до ~245–250 HV, то есть более чем в три раза. Полученные результаты подтверждают высокую эффективность наномодифицированного ПЭО-метода для повышения эксплуатационных свойств алюминиево-кремниевых сплавов.

Ключевые слова: плазменно-электролитическое оксидирование, алюминиево-кремниевый сплав, ПЭО-покрытие, наночастицы Al_2O_3, наночастицы SiO_2, микроструктура, микротвердость

References

1 Yeshmanova, G.B., Smagulov, D.U., & Blawert, C. (2021). Plasma electrolytic oxidation technology for producing protective coatings of aluminum alloys. *Complex use of mineral resources, 317*(2), 78–93. https://doi.org/10.31643/2021/6445.21.

2 Sowa, M., Wala, M., Błacha-Grzechnik, A., Maciej, A., Kazek-Kęsik, A., Stolarczyk, A., & Simka, W. (2021). Corrosion inhibitor-modified plasma electrolytic oxidation coatings on 6061 aluminum alloy. *Materials, 14*(3), Article 619. https://doi.org/10.3390/ma14030619.

3 Dzhurinskiy, D.V., Dautov, S.S., Shornikov, P.G., & Akhatov, I.S. (2021). Surface modification of aluminum 6061-O alloy by plasma electrolytic oxidation to improve corrosion resistance properties. *Coatings, 11*(1), Article 4. https://doi.org/10.3390/coatings11010004.

4 Peng, Z., Xu, H., Liu, S., Qi, Y., & Liang, J. (2021). Wear and corrosion resistance of plasma electrolytic oxidation coatings on 6061 Al alloy in electrolytes with aluminate and phosphate. *Materials, 14*(14), Article 4037. https://doi.org/10.3390/ma14144037.

5 Famiyeh, L., & Huang, X. (2019). Plasma electrolytic oxidation coatings on aluminum alloys: Microstructures, properties, and applications. *Modern Concepts in Material Science, 2*(1), Article 000526. https://doi.org/10.33552/MCMS.2020.02.000526.

6 Egorkin, V.S., Vyaliy, I.E., Sinebryukhov, S.L., & Gnedenkov, S.V. (2015). Formirovanie tverdykh, iznosostoikikh PEO-pokrytii na splave aliuminiia AMg3 [Formation of the hard, wear-resistant PEO-coatings on aluminum alloy AMg3]. *Vestnik Dalnevostochnogo otdeleniia Rossiiskoi akademii nauk — Vestnik of the Far East Branch of the Russian Acsdemy of Sciences*, 4, 53–61. Retrieved from https://cyberleninka.ru/article/n/formirovanie-tverdyh-iznosostoykih-peo-pokrytiy-na-splave-alyuminiya-amg3.

7 Nadimi, M., Dehghanian, C., & Etemadmoghadam, A. (2022). Influence of SiO_2 nanoparticles incorporating into ceramic coatings generated by PEO on aluminium alloy: Morphology, adhesion, corrosion, and wear resistance. *Materials Today Communications*, *31*, 103587. https://doi.org/10.1016/j.mtcomm.2022.103587

8 Uazyrkhanova, G., Sagidugumar, A., Kozhakhmetov, Y., Moldabayeva, G., Kaliyev, D., Rudenko, S., & Kantay, N. (2025). High-frequency plasma electrolytic oxidation of an Al–Si alloy: Influence of Al_2O_3 and SiO_2 additives on coating microstructure and tribological performance. *Materials, 18*(23), Article 5334. https://doi.org/10.3390/ma18235334.

9 Lu, X., Mohedano, M., Blawert, C., Matykina, E., Arrabal, R., Kainer, K.U., & Zheludkevich, M.L. (2016). Plasma electrolytic oxidation coatings with particle additions — A review. *Surface and Coatings Technology, 307* (Part C), 1165–1182. https://doi.org/10.1016/j.surfcoat.2016.08.055.

10 Kozlov, I.A., Vinogradov, S.S., Tarasova, K.G., Kulyushina, N.V., & Manchenko, V.A. (2019). Plazmennoe elektrolitcheskoe oksidirovanie magnievykh splavov (obzor) [Plasma electrolytic oxidation of magnesium alloys (review)]. *Aviatsionnye materialy i tekhnologii — Aviation Materials and Technologies*, 1(54), 23–36. https://doi.org/10.18577/2071-9140-2019-0-1-23-36.

11 Yerokhin, A.L., Nie, X., Leyland, A., Matthews, A., & Dowey, S.J. (1999). Plasma electrolysis for surface engineering. *Surface and Coatings Technology, 122*, 73–93. https://doi.org/10.1016/S0257-8972(99)00441-7.

12 Popova, N.A., Nikonenko, E.L., Tabieva, E.E., Uazyrkhanova, G.K., & Gromov, V.E. (2020). Influence of surface quenching on morphology and phase composition of ferritic–pearlitic steel. *Izvestiia. Ferrous Metallurgy, 63*(11-12), 915–921. https://doi.org/10.17073/0368-0797-2020-11-12-915-921.

13 Kombayev, K., Khoshnaw, F., Uazyrkhanova, G., & Moldabayeva, G. (2024). Experimental and mathematical modelling investigation of plasma electrolytic oxidation (PEO) for surface hardening of 20Ch steel. *Materials, 17*(24), Article 6043. https://doi.org/10.3390/ma17246043.

14 Kombayev, K., Kim, A., Sypainova, G., & Yelemanov, D. (2023). Improving wear resistance by electrolyte-plasma hardening of corrosion-resistant steel of the tip. *Journal of Applied Engineering Science, 21*(3), 810–819. https://doi.org/10.5937/jaes0-42291.

15 Fernández-López, P., Alves, S.A., San-Jose, J.T., Gutierrez-Berasategui, E., & Bayón, R. (2024). Plasma electrolytic oxidation (PEO) as a promising technology for the development of high-performance coatings on cast Al–Si alloys: A review. *Coatings, 14*(2), Article 217. https://doi.org/10.3390/coatings14020217.

Information about the authors

Kombayev, Kuat — Candidate of Technical Sciences, Associate professor, D. Serikbayev East Kazakhstan Technical University, Serikbayev Street, 19, Ust-Kamenogorsk, Kazakhstan; e-mail: kkombaev@edu.ektu.kz; ORCID ID https://orcid.org/0000-0002-6929-2748

Moldabayeva, Gulzhaz (*corresponding author*) — Doctoral student, D. Serikbayev East Kazakhstan Technical University, Serikbayev Street, 19, Ust-Kamenogorsk, Kazakhstan; e-mail: gmoldabaeva@edu.ektu.kz; ORCID ID https://orcid.org/0000-0001-9192-7087

Kozhakhmetov, Yernat — PhD, Head of the Center of Excellence "VERITAS", D. Serikbayev East Kazakhstan Technical University, Serikbayev Street, 19, Ust-Kamenogorsk, Kazakhstan; e-mail: ykozhakhmetov@edu.ektu.kz; ORCID ID https://orcid.org/0000-0002-6778-1898

Uazyrkhanova, Gulzhaz — PhD, Director of the Department of Research Activities, D. Serikbayev East Kazakhstan Technical University, Serikbayev Street, 19, Ust-Kamenogorsk, Kazakhstan; e-mail: guazyrhanova@edu.ektu.kz; ORCID ID https://orcid.org/0000-0002-9817-9752

Tabiyeva, Yerkezhan — PhD, Leading Researcher, Senior Lecturer, D. Serikbayev East Kazakhstan Technical University, Serikbayev Street, 19, Ust-Kamenogorsk, Kazakhstan; e-mail: etabieva@edu.ektu.kz; ORCID ID https://orcid.org/0000-0002-9726-7187

Kakimzhanov, Dauir — Doctoral student, D. Serikbayev East Kazakhstan Technical University, Serikbayev Street, 19, Ust-Kamenogorsk, Kazakhstan; e-mail: d.kakimzhanov19@gmail.com; ORCID ID https://orcid.org/0000-0001-9453-0456